J Mater Sci: Mater Electron (2021) 32:22245–22255

Synergistic approach of high-performance N-NiCo/PC environment benign electrode material for energy storage device

Muhammad Irfan[1], Xianhua Liu[1,*], Halayit Gebreselassie Abrha[1], Jonnathan Cabrera[1], Suraya Mushtaq[1], Yexin Dai[1], and Pingping Zhang[2]

[1] School of Environmental Science and Engineering, Tianjin University, Tianjin 300354, People's Republic of China
[2] College of Food Science and Engineering, Tianjin Agricultural University, Tianjin 300384, People's Republic of China

Received: 20 January 2021
Accepted: 25 July 2021
Published online: 3 August 2021

ABSTRACT

The development of sustainable electrochemical energy storage devices faces a great challenge in exploring highly efficient and low-cost electrode materials. Biomass waste-derived carbonaceous materials can be used as an alternative to expensive metals in supercapacitors. However, their application is limited by low performance. In this study, the combination use of persimmon waste-derived carbon and transition metal nitride demonstrated strong potential for supercapacitor application. Persimmon-based carbonaceous gel decorated with bimetallic nitride (N-NiCo/PC) was firstly synthesized through a green hydrothermal method. Electrochemical properties of N-NiCo/PC electrode in 6 M KOH electrolyte solution were evaluated using cyclic voltammetry (CV) and charge–discharge measurements. The N-NiCo/PC exhibited 320 F/g specific capacitance at 1 A/g current density and maintained 91.4% capacitance retention after 1500 cycles. Additionally, it exhibited a high energy density of 29.44 Wh/kg at 1000 W/kg power density and sustained 5.5 Wh/kg energy density even at a power density of 10,000 W/kg. Hence, the bimetallic nitride-based composite catalyst is a potentially suitable material for high-performance energy storage devices. In addition, this work demonstrated a promising pathway for transforming environmental waste into sustainable energy conversion materials.

1 Introduction

Recently, there is a need to protect natural resources and control energy consumption because of global warming. With rapid population growth, the energy demand can be attained in the direction of unconventional sustainable and renewable energy devices [1], like fuel cells [2–5], batteries [6], and supercapacitors [7] that can convert chemically stored energy into electrical energy through electrochemical

Address correspondence to E-mail: lxh@tju.edu.cn

https://doi.org/10.1007/s10854-021-06709-5

reactions. Among these different technologies, the supercapacitor has received great attention because of its high power density, good cycle stability, fast storage capacity, and excellent operational safety [8]. According to its energy storage mechanism, a supercapacitor can be divided into a pseudo-capacitor and an electric double-layer capacitor. The capacitance of the pseudo-capacitor comes from the reversible faraday redox reaction of electroactive material at the electrode interface and electrolyte. The capacitance of electric double-layer capacitor is caused by the accumulation of pure electrostatic charge at the electrode/electrolyte interface and it has more stable reversible electrochemical performance and longer cycle life than pseudo-capacitors because of these properties it grabbed researcher's intention in last few decades [9]. However, supercapacitor performance based on the electrode material selection, the material having large specific surface area and good electrical conductivity is considered suitable for high-performance supercapacitor [10, 11]. In various energy devices, carbon is the mainstream active component owing to its low cost, good conductivity, magnificent stability, and simple fabrication design. So far, porous carbon materials such as activated carbon (AC) [12], graphene [13], carbon nanotubes (CNT) [14], and biomass-derived carbon hydro-aerogel [15–17] have provoked wide range utilization in energy storage systems. Commercially fabrication of energy storage devices largely depends on abundant electrode material resources, economical, eco-friendly, and sustainable manufacturing. These well-designed carbons are usually complex to synthesize, costly, and agglomeration are obstacles in their applied application. With rapid economic development, we still face many challenges. It has become a key issue to explore economical and effective electrode materials with excellent electrochemical performance. In this regard, biomass-based hydro-aerogels are a good candidate in energy storing systems.

The efficiency-stability of the hydro-aerogel-based electrode can be enhanced with the addition of metals and their oxides. The cost-effective transition metals (TM) or metal oxides demonstrated comparable performance to noble metals and have attained enormous interest recently. In supercapacitor application the transition metals, nickel (Ni) [18], cobalt (Co) [19], ruthenium (Ru) [20], vanadium (V) [21], and manganese (Mn) [22], are widely used because of their high faradic charge transference process [23]. To improve metal's conductance and sustainability, the combination of transitional metals and nitrides is widely applied in supercapacitors [24]. Conductive TM provides a combination of electronic conductance, valance state diversity, and sustainability-like unique properties and is a potential candidate for energy storage systems in comparison with equivalent metals or metallic oxides [25–27]. Additionally, the presence of nitrogen strongly affects the electronic properties of the metal by increasing the electron density on the metal surface [2].

In the work presented here, we synthesized a material N-NiCo decorated on the persimmon waste carbonaceous gel (PC) through a simple glass route method. The as-prepared composite material N-NiCo/PC was applied in the supercapacitor. The use of bimetallic transition metals along with nitride provides a renewable green synthetic route for catalytic carbon material for the electrode. The use of bimetallic PC along with nitride provides a renewable green synthetic method for high-performance supercapacitor.

2 Experiment section

2.1 Preparation of persimmon fruit waste aerogel and N-NiCo/PC

Scheme 1 represents the synthesis procedure for N-NiCo/PC composite material. Briefly, the persimmon fruit waste was collected and washed with distilled water. The fruit was shacked and autoclaved at 150 °C using 100 mL Teflon vessels for 10 h. After being naturally cooled the block of hydrogel was removed from the vessels and kept in ethanol solution for 3 days to get rid of impurities. The hydrogel block was cut into 1 cm^2 pieces and dried through vacuum freeze-drying. A brown-colored aerogel was obtained after being dried completely followed by annealing at 350 °C in a tube furnace for 4 h. The persimmon-based carbonaceous gel (500 mg) was soaked in an ethanol solution containing nickel nitride Ni $(NO_3)_2.6H_2O$, cobalt nitride Co $(NO_3)_2.6H_2O$ (molar ratio 1:1), and urea (H_2NCONH_2) and then stirred by nitrogen supply for 8 h. The soaking process continued for 8 h and after that the material was dried at 70 °C in a vacuum oven overnight. The dried composite material was then carbonized

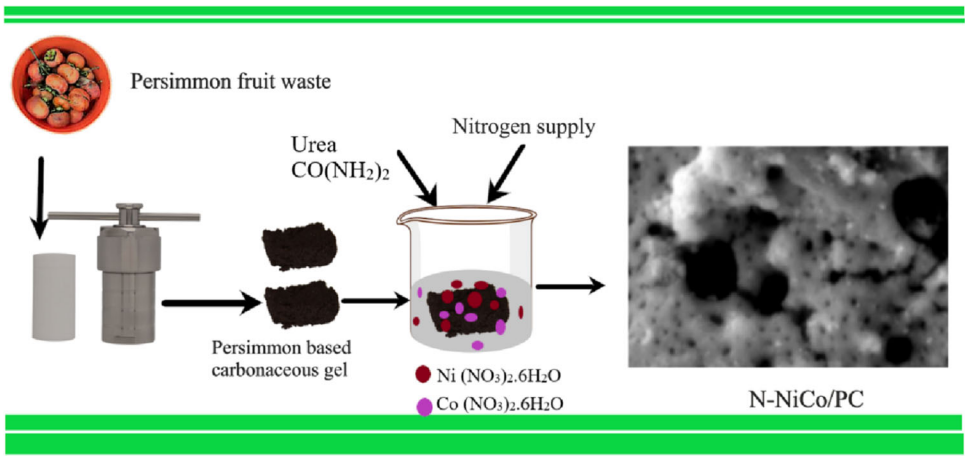

Scheme 1 The schematic diagram for the preparation of the N-NiCo/PC composite sample

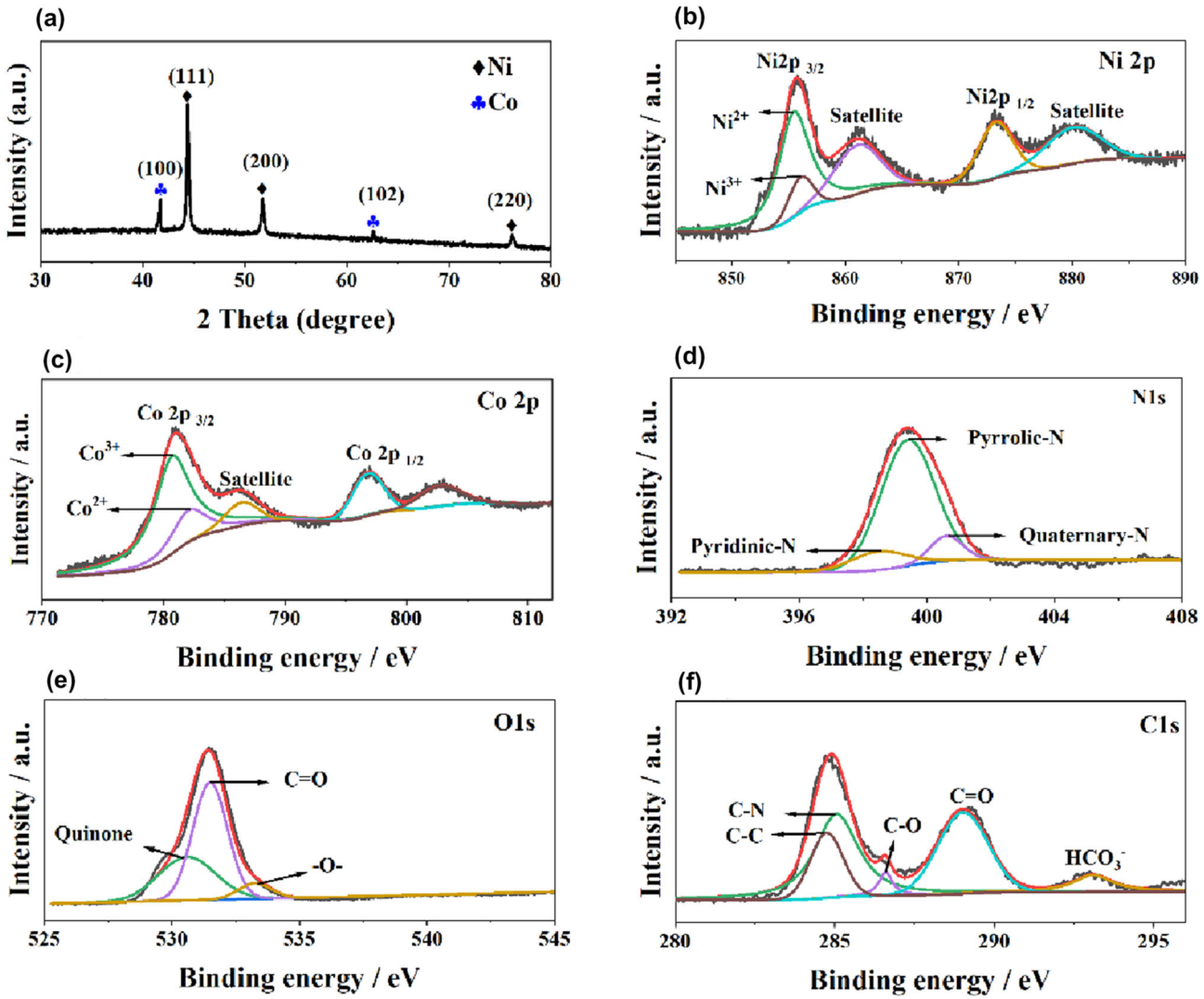

Fig. 1 Physical characterization by XRD and XPS of N-NiCo/PC composite material. **a** XRD; **b** Ni 2p; **c** Co 2p; **d** N1s; **e** O1s; **f** C1s

through a tube furnace at 350 °C for 5 h under a nitrogen environment. The tube furnace was naturally cooled down and the obtained persimmon-based carbonaceous gel was decorated with bimetallic nitride (N-NiCo/PC) composite and then used for electrode preparation. N-Ni/PC and N-Co/PC were also prepared for comparison by following the same procedure.

2.2 Physical and electrochemical characterization

The XRD, XPS, FE-SEM, and EDAX spectra were used for the physical characterization of the bimetallic nitride composite material. The electrochemical characterization was achieved using CHI 660E electrochemical workstation (CH Instruments, Inc. Shanghai). An electrode was fabricated by loading N-NiCo/PC, carbon black, and PTFE (80:1:1) on HCL-cleaned nickel foam. The fabricated electrode was dried overnight and pressed. 6 M KOH solution was used for three-electrode systems: (1) N-NiCo/PC working electrode; (2) Pt counter electrode; (3) Hg/HgO reference electrode, respectively. The other electrodes, N-Ni/PC and N-Co/PC, were synthesized following the same methodology. The specific capacitance of synthesized electrodes was obtained through cyclic voltammetry (CV) and charge–discharge measurements using the following equations:

$$C_{sp} = \frac{\int i dV}{v.\Delta V.m} \quad (1)$$

$$C_{sp} = \frac{I\Delta t}{m\Delta V} \quad (2)$$

where $\int \rangle dV$ represent the area under the CV curve, ΔV represent the potential window, m indicates the loading material (mg), v indicates the scan rate (mV/s), I indicate the discharge current density (A), and Δt represent the discharge time (s), respectively.

The specific capacitance from charge to discharge, power (P)W/kg, and energy density (E)Wh/kg of the two-electrode supercapacitor was calculated using Eqs. (3, 4, 5) [28]:

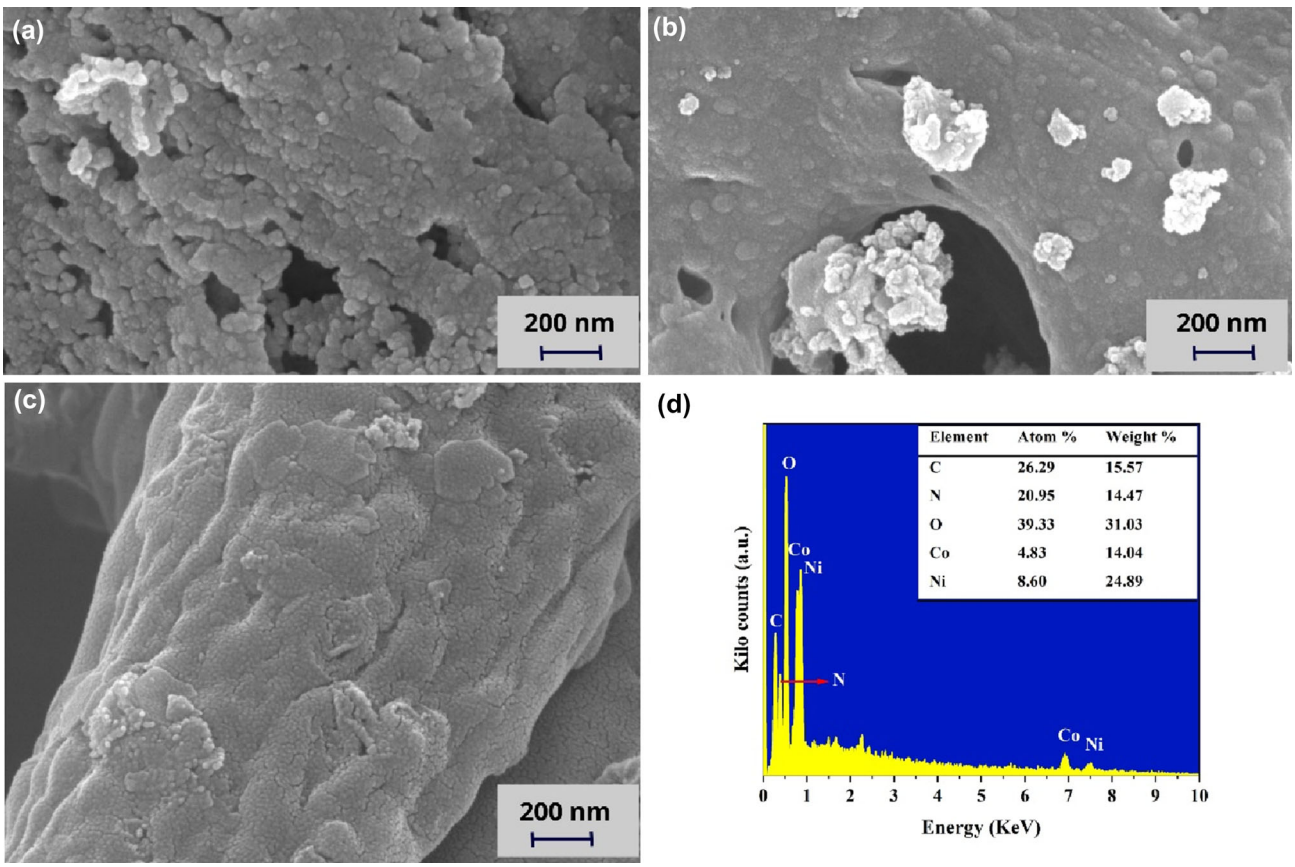

Fig. 2 FE-SEM images of **a** N-Ni/PC; **b** N-Co/PC; **c** N-NiCo/PC, and **d** the EDAX spectrum of N-NiCo/PC

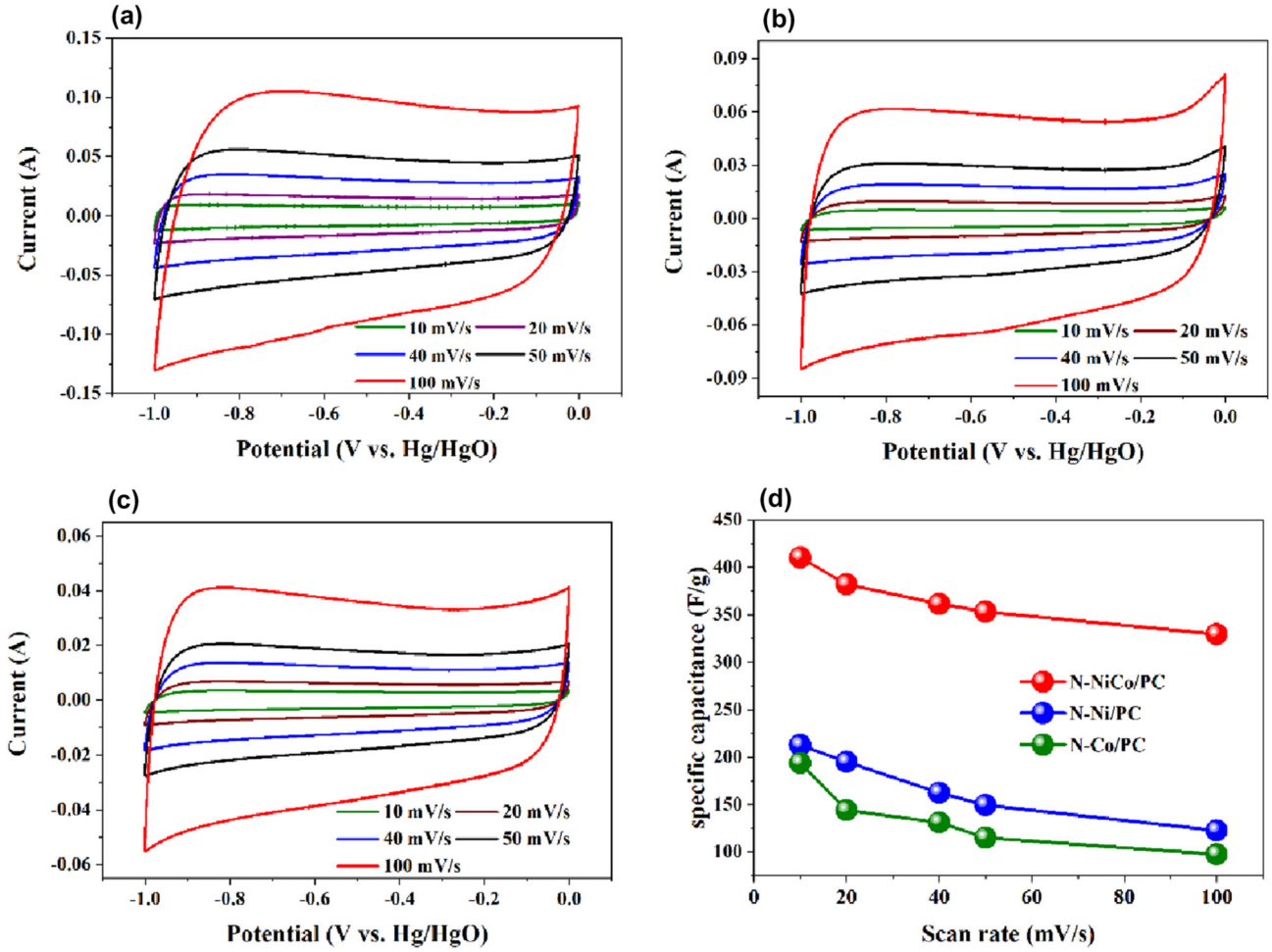

Fig. 3 The cyclic voltammetry of three composite materials at various scan rates; **a** N-NiCo/PC; **b** N-Ni/PC; **c** N-Co/PC; **d** specific capacitances of the above-mentioned electrodes

$$C_s = \frac{4It}{m\Delta V}, \tag{3}$$

$$E = \frac{C_s \Delta V^2}{2} \times \frac{1}{3600}, \tag{4}$$

$$P = \frac{E}{t}3600. \tag{5}$$

3 Results and discussion

Figure 1a shows the XRD pattern of synthesized composite material N-NiCo/PC. The characteristic peaks of metallic nickel and cobalt appeared in the XRD pattern, revealed the phase purity of the prepared material. The diffraction peaks at 44.39° (111), 51.71° (200), and 76.17° (220) attributed to metallic nickel, while the peaks appeared at 41.72° (100) and 62.74° (102) correspond to metallic cobalt, respectively [29]. Further, the valance state and chemical composition of the N-NiCo/PC was characterized through XPS (Fig. 1b–f). The Ni 2p indicates peaks at the binding energies of 855.5 eV and 873.25 eV which correspond to Ni $2p_{1/2}$ and Ni $2p_{3/2}$, respectively [4]. In addition, the deconvoluted peak centered at 856.9 can be assigned to Ni^{3+} [30]. The presence of Ni^{3+} peak may preclude further surface oxidation and Ni^{3+} state is considered more electroactive than Ni^{2+} state which can be beneficial to promote electrons transportation [30, 31]. In the Co 2p, two peaks appeared that correspond to Co $2p_{3/2}$ and Co $2p_{1/2}$ and accompanied a couple of satellites, representing the presence of Co^{2+} and Co^{3+} states

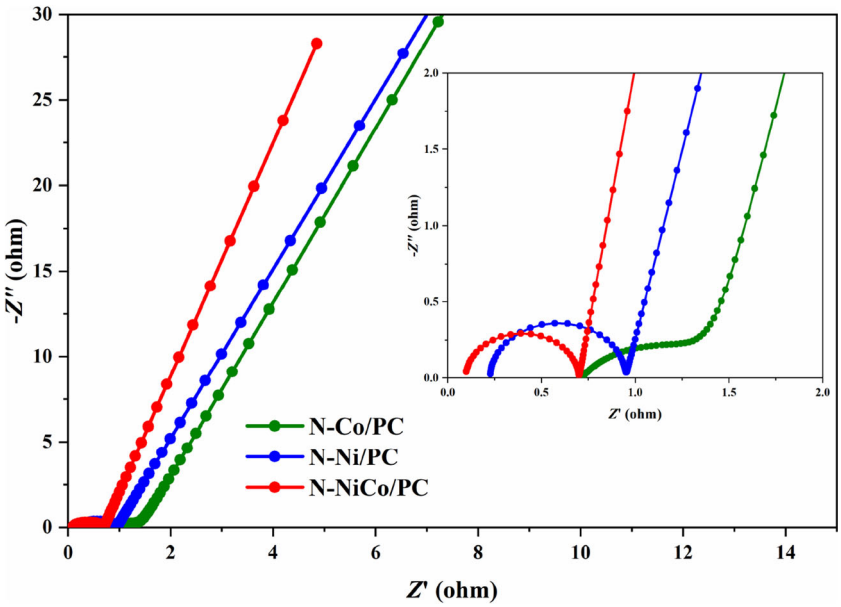

Fig. 4 Nyquist plot of N-Ni/PC, N-Co/PC, and N-NiCo/PC electrodes fitted by an equivalent electrical circuit

Table 1 Supercapacitor-fitted EIS data for N-Ni/PC, N-Co/PC, and N-NiCo/PC electrodes by an equivalent electrical circuit

Supercapacitor electrode	R_s (Ω)	R_{ct} (Ω)	R_d (Ω)	R_t (Ω)
N-NiCo/PC	0.0642	0.589	0.6223	1.2755
N-Ni/PC	0.0765	0.781	0.8351	1.6926
N-Co/PC	0.7137	0.838	0.7137	2.2651

[30]. The pyridinic N, pyrrolic N, and Quaternary N peaks appeared at binding energies of 398.5 ± 0.2, 399.4 ± 0.2, and 400.65 ± 0.2 eV, respectively, and are considered as faradaic-active species and can improve electron transport, surface wettability, and ion transport from the electrolyte to interface [2, 32]. There are three peaks observed in the O1s spectra at a binding energy of 530.50 ± 0.2, 531.5 ± 0.2, and 53.4 ± 0.2 eV, which correspond to quinone, carboxyl, and single bond oxygen, respectively. The oxygen-based groups can increase wettability, reduce resistance, improve electrochemical property, and react with hydrogen ions reversibly in an alkaline environment [2]. The C1s spectrum can be deconvoluted into five peaks corresponding to C–C (284.2 ± 0.2 eV), C–N (285.05 ± 0.2 eV), C–O (286.65 ± 0.2), C = O (289 ± 0.2), and HCO_3^- (293 ± 0.2), respectively.

The morphology of the obtained composite material was analyzed using FE-SEM. Figure 2a–c represents the FE-SEM images at a 200 nm diameter of N-Ni/PC, N-Co/PC, and N-NiCo/PC. The N-Ni/PC shows similar interconnected network channels on the carbonaceous gel surface that enables the diffusion and ion movements. However, large-sized cavities and aggregation of particles can be seen in the N-Co/PC composite material. As for N-NiCo/PC, many small-sized nanoparticles and cracks are uniformly distributed which may be beneficial for the electrochemical reactions. The EDAX spectra (Fig. 2d) showed the presence of C, N, O, Co, and Ni elements in the N-NiCo/PC. Their compositions are C (15.57 wt%), O (31.03 wt%), N (14.47 wt%), Ni (24.89 wt%), and Co (14.04 wt%).

The performance of annealed composite catalysts analyzed in supercapacitor. The black slurry (see methodology section) contained catalysts N-Ni/PC, N-Co/PC, and N-NiCo/PC used as the working electrode. Cyclic voltammogram (CV) and galvanostatic charge–discharge characterization were carried out within − 1.0 to 0 V potential window in 6 M KOH solution. Figure 3a–c shows that the CV curve of three annealed catalysts measured at various scan rates (mV/s) has an asymmetric shape which could be due to pseudocapacitance behavior. It can be seen from the CV profile that the area under the N-NiCo/PC CV curve is superior to that of N-Ni/PC and N-Co/PC nanostructures. The specific capacitance calculated at different scan rates is presented in Fig. 3d. The C_{sp} of N-NiCo/PC is 410 and 329.5 (F/g), at the scan rates of 10–100 mV/s, respectively. The improvement in the performance of N-NiCo/PC may be due to the reduction in crystal size, mesoporous structure, and high surface area allowing ions to

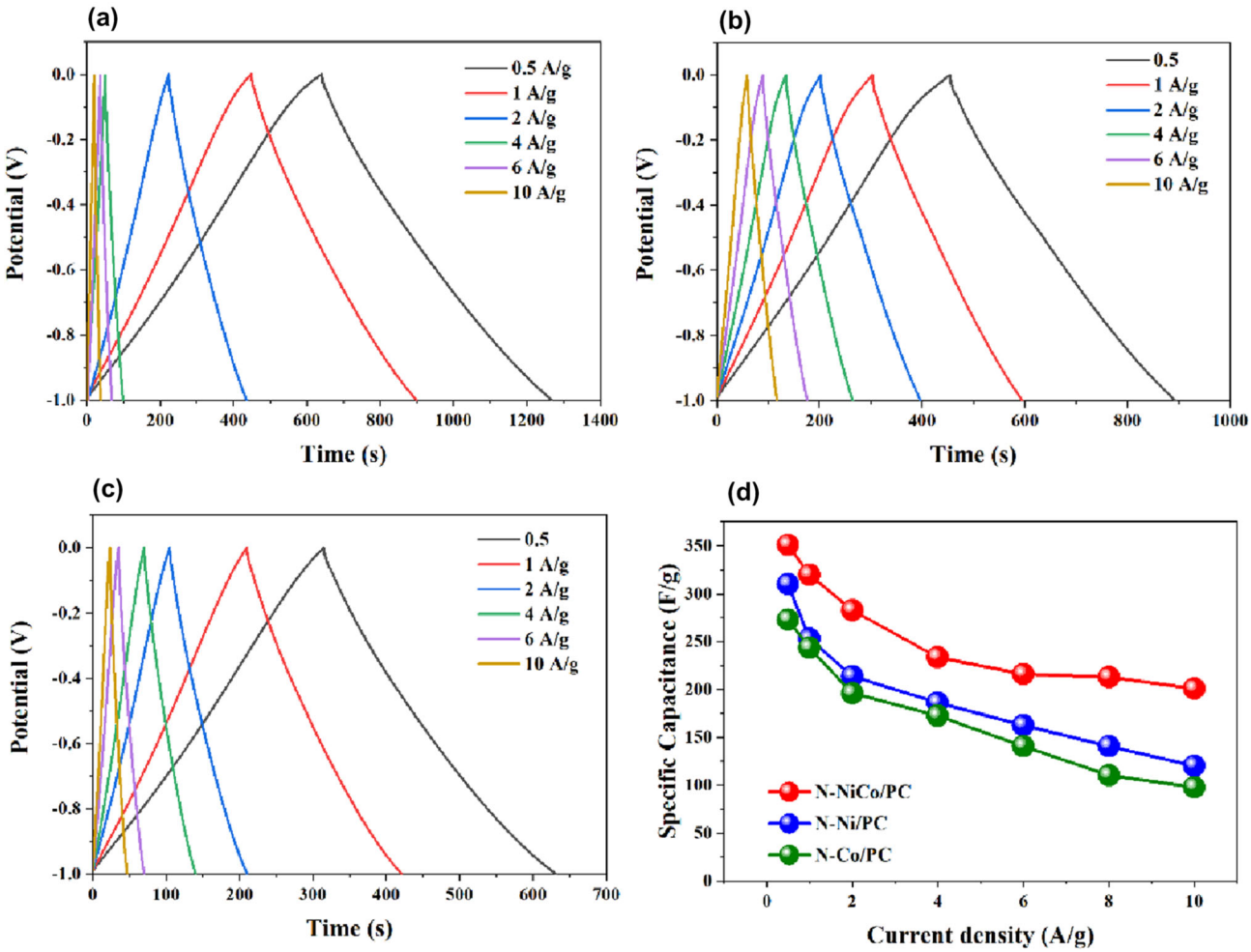

Fig. 5 The charge–discharge behavior of composite catalysts at various current densities; **a** N-NiCo/PC; **b** N-Ni/PC; **c** N-Co/PC, and the specific capacitance of charge–discharge **d** comparison of N-NiCo/PC, N-Ni/PC, and N-Co/PC

rapidly enter the active site of the electrode [33]. The smaller the grain size, the larger the surface volume ratio and the stronger the charge storage capacity of the electrode.

EIS was determined to demonstrate the excellent electrochemical performance of N-NiCo/PC supercapacitor electrode as shown in Fig. 4. R_s electrodes are measured at 0.06429 Ω, 0.0.0765 Ω, and 0.7137 Ω, respectively, indicating the goodness of N-NiCo/PC electrodes' electrical conductivity. The semicircle is in the high frequency range corresponds to R_{ct} (charge transfer) resistance (Table 1) caused by the Faraday reaction. The charge transfer resistance of the N-NiCo/PC electrode is lower due to its higher surface area and uniform distribution of nickel nanoparticles providing a more active reaction site, indicating that the electrode material as a supercapacitor has a higher electrochemical reactivity. Additionally, N-NiCo/PC has a relatively higher oxygen and nitride functional group that increased the electrode surface wettability resulting in a reduction in contact resistance [9]. The electrochemical properties of the supercapacitor consistent with the fuel cell indicate that N-NiCo/PC is applicable in both energy conversion and energy storage systems.

The charge and discharge behavior of three synthesized catalysts was also determined at 0.5–10 A/g current density. The triangular charge/discharge curve with slight internal resistance (*IR*) is shown in Fig. 5a–c, which implies a high degree of symmetry of charge/discharge. In beginning, the *IR* drop is usually associated with *ESR* (equivalent series resistance) phenomenon. The specific capacitance of these catalysts is calculated by the equation $C_{sp} = I\Delta t/m\Delta V$, where, C_{sp} is the specific capacitance of charge and discharge, constant charge/discharge

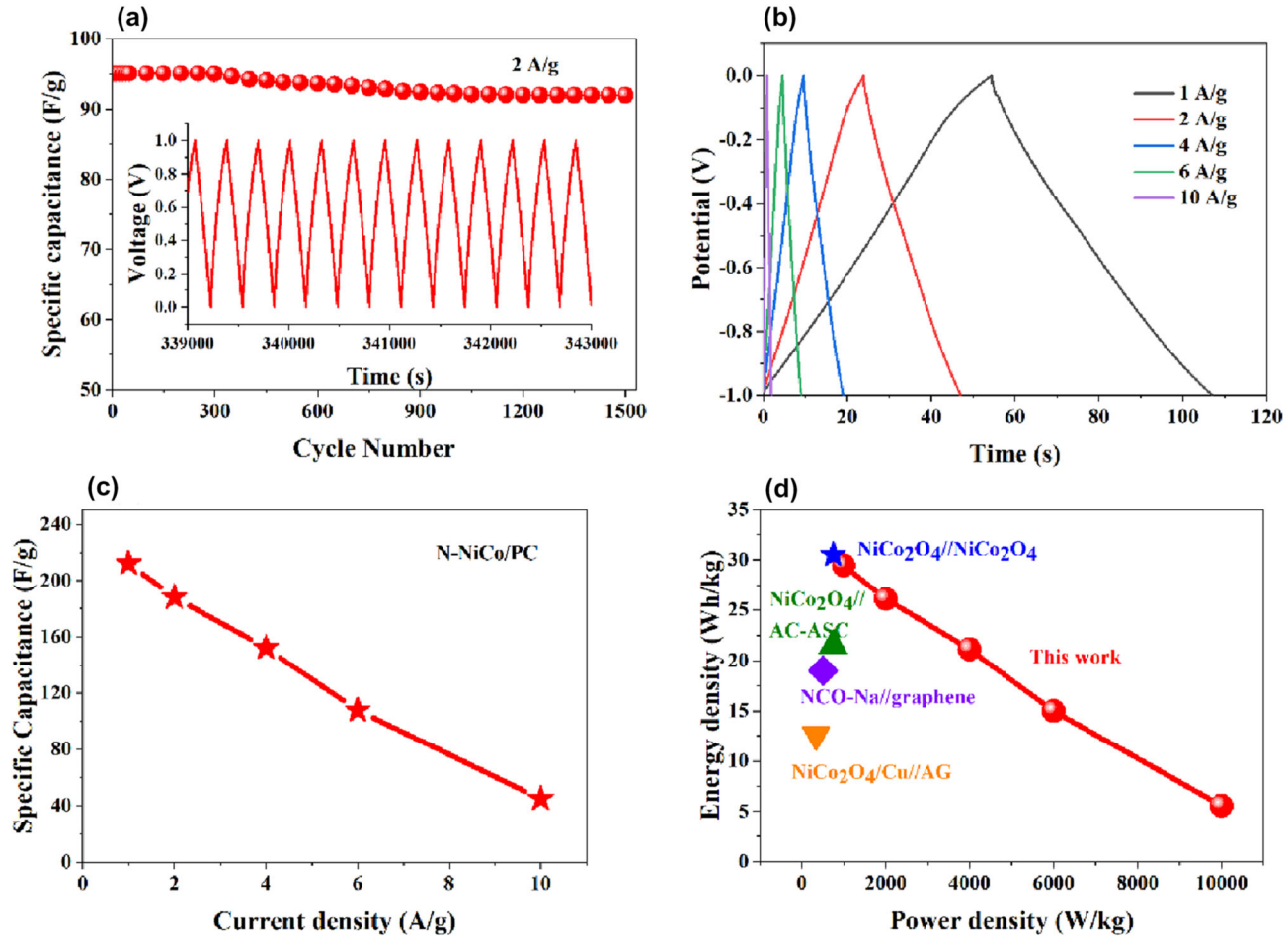

Fig. 6 Cycle's stability (1500 cycles) of N-NiCo/PC composite material **a** at 2 A/g current density; **b** charge–discharge curves of two electrodes N-NiCo/PC symmetric supercapacitor; **c** specific capacitance of charge–discharge; **d** Ragone plots of N-NiCo/PC device and other different material-based supercapacitors

current (A) is I, discharging time (s) is Δt, (m) mass of active material used and the potential window is ΔV [34]. The specific capacitance of N-NiCo/PC catalyst is 13.22% higher than N-Ni/PC, while it is 28.57% higher than N-Co/PC at a specific current of 0.5 A/g. Further, the charge and discharge behavior of N-NiCo/PC was analyzed at current densities from 1 to 10 A/g (Fig. 5d). The estimated specific capacitance is 320 and 283 F/g at current density 1 to 2 A/g, respectively. The specific capacitance obtained at 1 A/g is comparable to Fe_3O_4/graphene nanosheets (358 F/g) [35] and much higher than many composite materials like N doping of carbon fiber (202.0 F/g) [36], CeCoO3 (112 F/g) [37], NiCu hydro-oxide @ Ni–Cu–Se (158.95 F/g) [38], Ni-WO_3 (138.97 F/g)[39], and hollow graphite N-doped [36] carbon spheres (260 F/g). The excellent capacitive performance of the N-NiCo/PC is mainly due to its unique structure. Moreover, there are many active reaction sites on the surface, which can carry out more Faraday reactions; N-doped sites act as heteroatom defects, resulting in good conductivity, wettability of both electrode and electrolyte, resulting in rapid electron transfer, diffusion, and absorption rates [40–42].

The life cycle stability of the N-NiCo/PC electrode was evaluated by constant current charge and discharge at 2 A/g. Capacitance retention of N-NiCo/PC electrode during 1500 charge/discharge cycles test is shown in Fig. 6a. The capacitance retention throughout the cycle test is calculated by (each cycle ratio/first cycle capacitance value); in the first 500 cycles, 8.6% capacitance retention of the N-NiCo/PC electrode is lost with the increasing charge/discharge cycle and remains almost unchanged at 1500 cycles. Outstanding life cycle stability may result from a porous structure with the least crystallographic

changes during catalyst synthesis. Thus, good specific capacitance retention reflects the higher durability of N-NiCo/PC electrodes in excellent performance supercapacitor applications.

In addition, symmetrical supercapacitor based on N-NiCo/PC was assembled to evaluate in practical application. The charge–discharge curves at different current densities of as-assembled supercapacitor (Fig. 6b) showed triangular profiles suggesting an excellent charge–discharge capacitive response. Figure 6c represents specific capacitance derived from charge–discharge curves at various current densities 1, 2, 4, 6, and 10 A/g. Ragone plot represents the energy and power density of the N-NiCo/PC device (Fig. 6d). The N-NiCo/PC exhibited a high energy density of 29.44 Wh/kg at 1000 W/kg power density and the device sustained 5.5 Wh/kg energy density even at a power density of 10,000 W/kg. Such results are better than other previously reported symmetrical and asymmetrical devices [43–46]. All the above-mentioned results revealed that the N-NiCo/PC supercapacitor can deliver significant performance in comparison with the traditional electrode material.

4 Conclusion

In this paper, persimmon waste was used to synthesize an aerogel through the hydrothermal method. Then, nickel, cobalt, and nitride were introduced in aerogel and prepared N-NiCo/PC composite catalyst for supercapacitor electrode. The specific capacitance of N-NiCo/PC catalyst is 13.22% higher than N-Ni/PC, while it is 28.57% greater than N-Co/PC at a specific current of 0.5 A/g. After, 1500 cycles, our N-NiCo/PC electrode maintained 91.4% of its capacitance retention. Thus, from this finding, it could be concluded that the cost-effective bimetallic nitride electrode N-NiCo/PC has the potential for high-performance storage devices.

Author contributions

Investigation, Data curation, and Writing—original draft: [MI]; Conceptualization, Supervision, and Writing—review and editing [XL]; Material preparation [HGA]; Formal analysis and investigation [JC]; Formal analysis and investigation [SM]; Characterization [YD]; Conceptualization and Writing—review and editing [PZ].

Funding

This work was partially supported by the National Key R&D Program of China (Grant No. 2019YFC1407800) and the Natural Science Foundation of Tianjin City (Grant No. 19YFZCSN01130).

Data availability

Not applicable.

Code availability

Not applicable.

Declarations

Conflict of interest There are no conflicts of interest to declare.

References

1. M.M. Afzal, M.A. Khan, M.A.S. Hassan, A. Wadood, W. Uddin, S. Hussain, S.B. Rhee, A comparative study of supercapacitor-based STATCOM in a grid-connected photovoltaic system for regulating power quality issues. Sustainability **12**(17), 6781 (2020)
2. M. Irfan, I.U. Khan, J. Wang, Y. Li, X. Liu, 3D porous nanostructured Ni 3 N–Co 3 N as a robust electrode material for glucose fuel cell. RSC Adv. **10**(11), 6444–6451 (2020)
3. M. Irfan, X. Liu, S. Li, I.U. Khan, Y. Li, J. Wang, X. Wang, X. Du, G. Wang, P. Zhsng, High-performance glucose fuel cell with bimetallic Ni–Co composite anchored on reduced graphene oxide as anode catalyst. Renew. Energy **155**, 1118 (2020)
4. M. Gao, X. Liu, M. Irfan, J. Shi, X. Wang, P. Zhang, Nickle-cobalt composite catalyst-modified activated carbon anode for direct glucose alkaline fuel cell. Int. J. Hydrog. Energy **43**(3), 1805–1815 (2018). https://doi.org/10.1016/j.ijhydene.2017.11.114
5. F. Dong, X. Liu, M. Irfan, L. Yang, S. Li, J. Ding, Y. Li, I.U. Khan, P. Zhang, Macaroon-like FeCo2O4 modified activated carbon anode for enhancing power generation in direct glucose fuel cell. Int. J. Hydrog. Energy **44**(16), 8178–8187 (2019)

6. M.S. Javed, D. Zhong, T. Ma, A. Song, S. Ahmed, Hybrid pumped hydro and battery storage for renewable energy based power supply system. Appl. Energy **257**, 114026 (2020)
7. S. Zhai, H.E. Karahan, C. Wang, Z. Pei, L. Wei, Y. Chen, 1D supercapacitors for emerging electronics: current status and future directions. Adv. Mater. **32**(5), 1902387 (2020)
8. C.A. Okonkwo, T. Lv, W. Hong, G. Li, J. Huang, J. Deng, L. Jia, M. Wu, H. Liu, M. Guo, The synthesis of micromesoporous carbon derived from nitrogen-rich spirulina extract impregnated castor shell based on biomass self-doping for highly efficient supercapacitor electrodes. J. Alloys Compd. **825**, 154009 (2020)
9. H. Yang, X. Sun, H. Zhu, Y. Yu, Q. Zhu, Z. Fu, S. Ta, L. Wang, H. Zhu, Q. Zhang, Nano-porous carbon materials derived from different biomasses for high performance supercapacitors. Ceram. Int. **46**(5), 5811–5820 (2020). https://doi.org/10.1016/j.ceramint.2019.11.031
10. Y. Gao, S. Zheng, H. Fu, J. Ma, X. Xu, L. Guan, H. Wu, Z.-S. Wu, Three-dimensional nitrogen doped hierarchically porous carbon aerogels with ultrahigh specific surface area for high-performance supercapacitors and flexible micro-supercapacitors. Carbon **168**, 701–709 (2020)
11. A.M. Al-Enizi, M. Ubaidullah, J. Ahmed, T. Ahamad, T. Ahmad, S.F. Shaikh, M. Naushad, Synthesis of NiOx@ NPC composite for high-performance supercapacitor via waste PET plastic-derived Ni-MOF. Compos. Part B: Eng. **183**, 107655 (2020)
12. F. Cheng, X. Yang, S. Zhang, W. Lu, Boosting the supercapacitor performances of activated carbon with carbon nanomaterials. J. Power Sources **450**, 227678 (2020)
13. K. Krishnamoorthy, P. Pazhamalai, V.K. Mariappan, S. Manoharan, D. Kesavan, S.J. Kim, Two-dimensional siloxene-graphene heterostructure-based high-performance supercapacitor for capturing regenerative braking energy in electric vehicles. Adv. Funct. Mater. **31**, 2008422 (2020)
14. J. Han, H. Wang, Y. Yue, C. Mei, J. Chen, C. Huang, Q. Wu, X. Xu, A self-healable and highly flexible supercapacitor integrated by dynamically cross-linked electro-conductive hydrogels based on nanocellulose-templated carbon nanotubes embedded in a viscoelastic polymer network. Carbon **149**, 1–18 (2019)
15. S. Lin, F. Wang, Z. Shao, Biomass applied in supercapacitor energy storage devices. J. Mater. Sci. **56**, 1943–1979 (2020)
16. S.H. Reis GSd, Larsson, M. de Oliveira HPd, Thyrel, E.C. Lima, Sustainable biomass activated carbons as electrodes for battery and supercapacitors–a mini-review. Nanomaterials **10**(7), 1398 (2020)
17. D. Kobina Sam, E. Kobina Sam, X. Lv, Application of biomass-derived nitrogen-doped carbon aerogels in electrocatalysis and supercapacitors. ChemElectroChem **7**(18), 3695–3712 (2020)
18. H. Kim, S. Surendran, Y. Chae, H.Y. Lee, T.-Y. An, H.S. Han, W. Park, J.K. Kim, U. Sim, Fabrication of an ingenious metallic asymmetric supercapacitor by the integration of anodic iron oxide and cathodic nickel phosphide. Appl. Surf. Sci. **511**, 145424 (2020)
19. A.M. Zardkhoshoui, S.S.H. Davarani, Construction of complex copper-cobalt selenide hollow structures as an attractive battery-type electrode material for hybrid supercapacitors. Chem. Eng. J. **402**, 126241 (2020)
20. K. Mensah-Darkwa, C. Zequine, P.K. Kahol, R.K. Gupta, Supercapacitor energy storage device using biowastes: a sustainable approach to green energy. Sustainability **11**(2), 414 (2019)
21. Q. Gong, J. Lei, Design of a bidirectional energy storage system for a vanadium redox flow battery in a microgrid with SOC estimation. Sustainability **9**(3), 441 (2017)
22. S.S. Siwal, Q. Zhang, C. Sun, V.K. Thakur, Graphitic carbon nitride doped copper–manganese alloy as high–performance electrode material in supercapacitor for energy storage. Nanomaterials **10**(1), 2 (2020)
23. M.A.A. Mohd Abdah, N.H.N. Azman, S. Kulandaivalu, Y. Sulaiman, Review of the use of transition-metal-oxide and conducting polymer-based fibres for high-performance supercapacitors. Mater. Des. **186**, 108199 (2020)
24. S. Yuan, S.-Y. Pang, J. Hao, 2D transition metal dichalcogenides, carbides, nitrides, and their applications in supercapacitors and electrocatalytic hydrogen evolution reaction. Appl. Phys. Rev. **7**(2), 021304 (2020)
25. Y. Liu, Z. Zeng, R.K. Sharma, S. Gbewonyo, K. Allado, L. Zhang, J. Wei, A bi-functional configuration for a metal-oxide film supercapacitor. J. Power Sources **409**, 1–5 (2019)
26. M.S. Faber, M.A. Lukowski, Q. Ding, N.S. Kaiser, S. Jin, Earth-abundant metal pyrites (FeS2, CoS2, NiS2, and their alloys) for highly efficient hydrogen evolution and polysulfide reduction electrocatalysis. J. Phys. Chem. C **118**(37), 21347–21356 (2014)
27. M. Zhang, X. Li, J. Zhao, X. Han, C. Zhong, W. Hu, Y. Deng, Surface/interface engineering of noble-metals and transition metal-based compounds for electrocatalytic applications. J. Mater. Sci. Technol. **38**, 221–236 (2020)
28. H. Wei, H. Wang, A. Li, H. Li, D. Cui, M. Dong, J. Lin, J. Fan, J. Zhang, H. Hou, Advanced porous hierarchical activated carbon derived from agricultural wastes toward high performance supercapacitors. J. Alloys Compd. **820**, 153111 (2020)
29. J. López-Tinoco, R. Mendoza-Cruz, L. Bazán-Díaz, S.C. Karuturi, M. Martinelli, D.C. Cronauer, A.J. Kropf, C.L. Marshall, G. Jacobs, The preparation and characterization of

Co–Ni nanoparticles and the testing of a heterogenized Co–Ni/alumina catalyst for CO hydrogenation. Catalysts **10**(1), 18 (2020)

30. T. Deepalakshmi, D.T. Tran, N.H. Kim, K.T. Chong, J.H. Lee, Nitrogen-doped graphene-encapsulated nickel cobalt nitride as a highly sensitive and selective electrode for glucose and hydrogen peroxide sensing applications. ACS Appl. Mater. Interfaces **10**(42), 35847–35858 (2018)
31. H. Sun, Y. Ye, Z. Tian, S. Wu, J. Liu, C. Liang, Ni 3 + doped cobalt–nickel layered double hydroxides as high-performance electrode materials for supercapacitors. RSC Adv. **7**(77), 49010–49014 (2017)
32. W. Wu, Q. Zhang, X. Wang, C. Han, X. Shao, Y. Wang, J. Liu, Z. Li, X. Lu, M. Wu, Enhancing selective photooxidation through Co–Nx-doped carbon materials as singlet oxygen photosensitizers. ACS Catal. **7**(10), 7267–7273 (2017). https://doi.org/10.1021/acscatal.7b01671
33. M. Wang, J. Du, J. Zhou, C. Ma, L. Bao, X. Li, X. Li, Numerical evaluation of the effect of mesopore microstructure for carbon electrode in flow battery. J. Power Sources **424**, 27–34 (2019)
34. Z. Wang, J. Liu, X. Hao, Y. Wang, Y. Chen, P. Li, M. Dong, Enhanced power density of a supercapacitor by introducing 3D-interfacial graphene. New J. Chem. **44**(31), 13377–13381 (2020)
35. W. Zhang, F. Liu, Q. Li, Q. Shou, J. Cheng, L. Zhang, B.J. Nelson, X. Zhang, Transition metal oxide and graphene nanocomposites for high-performance electrochemical capacitors. Phys. Chem. Chem. Phys. **14**(47), 16331–16337 (2012)
36. L.-F. Chen, X.-D. Zhang, H.-W. Liang, M. Kong, Q.-F. Guan, P. Chen, Z.-Y. Wu, S.-H. Yu, Synthesis of nitrogen-doped porous carbon nanofibers as an efficient electrode material for supercapacitors. ACS Nano **6**(8), 7092–7102 (2012)
37. Q. Hu, B. Yue, H. Shao, F. Yang, J. Wang, Y. Wang, J. Liu, Facile syntheses of cerium-based CeMO3 (M = Co, Ni, Cu) perovskite nanomaterials for high-performance supercapacitor electrodes. J. Mater. Sci. **55**(20), 8421–8434 (2020). https://doi.org/10.1007/s10853-020-04362-7
38. V.T. Chebrolu, B. Balakrishnan, V. Raman, I. Cho, J.-S. Bak, K. Prabakar, H.-J. Kim, Co-electrodeposition of NiCu(OH)2@Ni-Cu-Se hierarchical nanoparticle structure for supercapacitor application with enhanced performance. Appl. Surf. Sci. **506**, 145015 (2020). https://doi.org/10.1016/j.apsusc.2019.145015
39. R.D. Kumar, Y. Andou, S. Karuppuchamy, Synthesis and characterization of nanostructured Ni-WO3 and NiWO4 for supercapacitor applications. J. Alloys Compd. **654**, 349–356 (2016). https://doi.org/10.1016/j.jallcom.2015.09.106
40. H.M. El Sharkawy, A.S. Dhmees, A. Tamman, S. El Sabagh, R. Aboushahba, N.K. Allam, N-doped carbon quantum dots boost the electrochemical supercapacitive performance and cyclic stability of MoS2. J. Energy Storage **27**, 101078 (2020)
41. B. Wang, Y. Ye, L. Xu, Y. Quan, W. Wei, W. Zhu, H. Li, J. Xia, Space-confined yolk-shell construction of Fe3O4 nanoparticles inside N-doped hollow mesoporous carbon spheres as bifunctional electrocatalysts for long-term rechargeable zinc–air batteries. Adv. Funct. Mater. **30**(51), 2005834 (2020)
42. Y. Zhou, M. Zhang, Q. Wang, J. Yang, X. Luo, Y. Li, R. Du, X. Yan, X. Sun, C. Dong, Pseudocapacitance boosted N-doped carbon coated Fe 7 S 8 nanoaggregates as promising anode materials for lithium and sodium storage. Nano Res. **13**(3), 691–700 (2020)
43. H. Fu, Y. Liu, L. Chen, Y. Shi, W. Kong, J. Hou, F. Yu, T. Wei, H. Wang, X. Guo, Designed formation of NiCo2O4 with different morphologies self-assembled from nanoparticles for asymmetric supercapacitors and electrocatalysts for oxygen evolution reaction. Electrochim. Acta **296**, 719–729 (2019)
44. K. Xu, J. Yang, J. Hu, Synthesis of hollow NiCo2O4 nanospheres with large specific surface area for asymmetric supercapacitors. J. Colloid Interface Sci. **511**, 456–462 (2018)
45. Z. Cao, C. Liu, Y. Huang, Y. Gao, Y. Wang, Z. Li, Y. Yan, M. Zhang, Oxygen-vacancy-rich NiCo2O4 nanoneedles electrode with poor crystallinity for high energy density all-solid-state symmetric supercapacitors. J. Power Sources **449**, 227571 (2020)
46. M. Kuang, Y.X. Zhang, T.T. Li, K.F. Li, S.M. Zhang, G. Li, W. Zhang, Tunable synthesis of hierarchical NiCo2O4 nanosheets-decorated Cu/CuOx nanowires architectures for asymmetric electrochemical capacitors. J. Power Sources **283**, 270–278 (2015)